

Meteorology of the Beaufort Sea

James E. Overland¹

Received 10 April 2008; revised 29 July 2008; accepted 18 December 2008; published 6 May 2009.

[1] The unique meteorology of the Beaufort Sea region is dominated by the presence of sea ice and a seasonal swing from a large heat loss in winter to a gain in summer. The primary determinant of this seasonal climate shift is the annual cycle of insolation from a maximum of 500 W/m² near the summer solstice to darkness in winter, as the Beaufort Sea lies north of Alaska and northwestern Canada beyond 72°N. Even though the Sun angle is low in summer, the length of daylight provides as much energy to the surface as anywhere on the planet. As summer progresses, relative absorption of insolation at the surface increases as the albedo decreases due to snow and ice melt and increased open water area. This annual cycle results in a change from a winter continental-like air mass similar to the adjacent land areas to a summertime marine air mass characterized by low cloud and fogs. In winter the region is also influenced by the polar atmospheric vortex with strong westerly winds centered in the stratosphere, whose presence is felt at the surface. Recent sea ice losses are changing the climatology of the region, with extended periods of increased temperatures through the autumn months.

Citation: Overland, J. E. (2009), Meteorology of the Beaufort Sea, *J. Geophys. Res.*, 114, C00A07, doi:10.1029/2008JC004861.

1. Introduction

[2] This paper represents a synthesis of past and recent understanding of Beaufort Sea meteorology. Although the basic concepts, such as the polar vortex and annual cycle of the arctic heat budget, have been qualitatively known for decades, the advent of satellite data, the arctic buoy program, and computer power necessary for spatial analyses now provide a more quantitative overview.

[3] Little was known about the central Beaufort Sea until the last 50 years. Coastal voyages were made by indigenous residents for the last 1000 years and major commercial whaling was undertaken starting in the late nineteenth century. While the Russians began their North Pole Drifting Stations in 1937, the 1950s, including the International Geophysical Year in 1958, was a critical time for systematic central Arctic observations, including atmospheric temperature soundings. A less well known but significant theoretical advance was the classification and operational use of basic atmospheric circulation patterns by Soviet scientists [Vangengeim, 1946], referred to as W (western), E (eastern), and C (meridional) as forerunners of the more recently defined Arctic Oscillation and meridional patterns [Overland *et al.*, 2008].

[4] By the 1960s to early 1970s there was sufficient information for major reviews of Arctic meteorology [Reed and Kunkel, 1960; Vangengeim and Laktionov, 1967; Hare, 1968; Vowinckel and Orvig, 1970]. Reed and Kunkel note the formation of a frontal zone in summer along the northern shores of Siberia, Alaska and Canada due to

land-sea contrasts; cyclones that originate in this zone frequently invade the central Arctic, providing a contribution toward lower pressures in summer. By analyzing upper airflow, Hare indicates that both atmospheric motion and mass fields in winter are consistent with a cold core polar vortex. This is shown by the shape of the 500 hPa geopotential height field being similar to that of the surface to 500 hPa geopotential thickness field.

[5] More recent improvements in understanding of Arctic climate are based on the expanded coverage of sea level pressure and temperatures provided through the Arctic Buoy Program starting in 1979, and the observations from satellites in the 1970s and beyond. Given the starting time of buoy coverage, we make use of the NCEP-NCAR Reanalysis fields starting in 1979 and running through 2007 as the basis for our analyses. These sea level pressure and temperature fields are in good agreement with observational data [Makshtas *et al.*, 2007]. The SHEBA expedition in 1997–1998 provided a large range of in situ observations over a full year, which are representative of the seasonal cycle in the central Beaufort Sea [Uttal *et al.*, 2002]. This paper provides a discussion of the processes that determine the unique range of meteorological conditions of the Beaufort Sea, rather than providing a strict climatology of regional seasonal distributions of major atmospheric variables, as these are found elsewhere [Frolov *et al.*, 2005; Serreze and Barry, 2006].

2. Climatological Fields

[6] The basic driver of Beaufort Sea meteorology is the annual cycle of insolation (Figure 1). Although the Sun is close to the horizon during summer, the 24 h of daylight provides more potential solar radiation (i.e., without cloud

¹Pacific Marine Environmental Laboratory, NOAA, Seattle, Washington, USA.

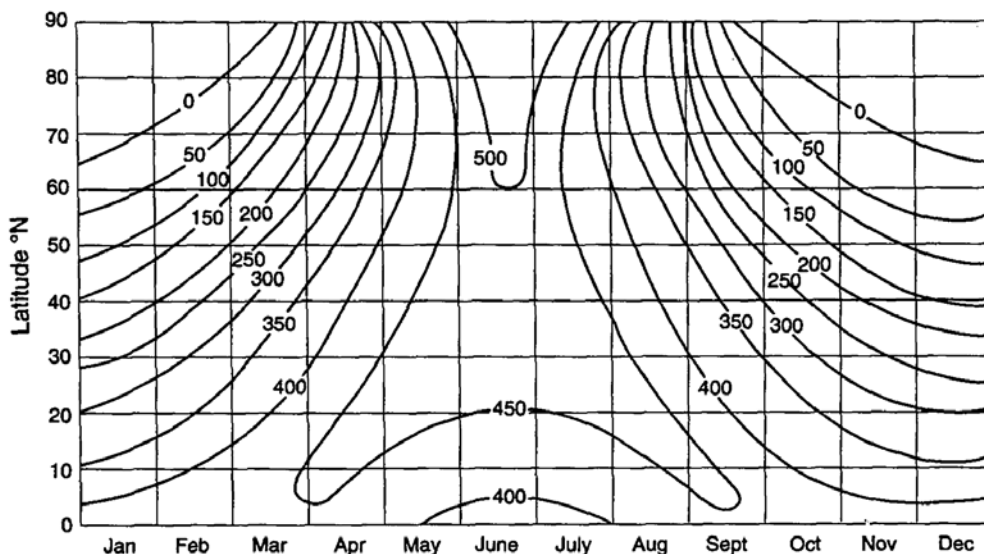


Figure 1. Latitudinal distribution of potential insolation for the Northern Hemisphere. Units are in W/m^2 .

effects) in the Arctic than at lower latitudes in the northern hemisphere.

[7] Sea level pressure (SLP) fields for the four seasons: winter (JFM), spring (AMJ), summer (JAS) and autumn (OND) are plotted in Figure 2, as indicators of the mean wind patterns and the tendency for clear or cloudy air masses based on high or low pressures. We assign these

months as an appropriate division for the seasons as extremes of Arctic surface conditions lag the traditional calendar. The Beaufort Sea lies to the north of the region of strongest easterly winds, noted by large pressure gradients over Alaska in three of the four seasons. In the vertical plane the Arctic is generally considered a region of downward motion as the northern arm of the “Ferrel Cell,” but

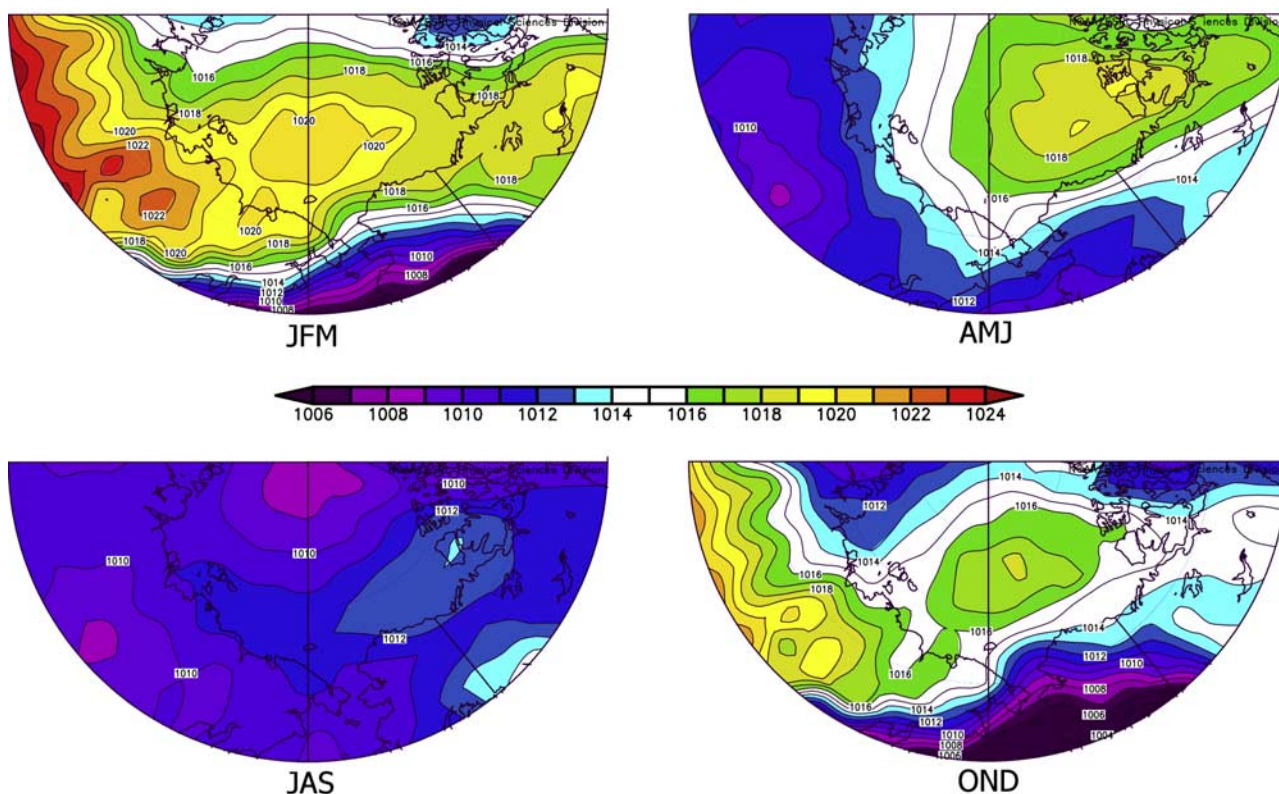


Figure 2. Mean (1979–2007) sea level pressure for the four seasons over the greater Beaufort Sea region.

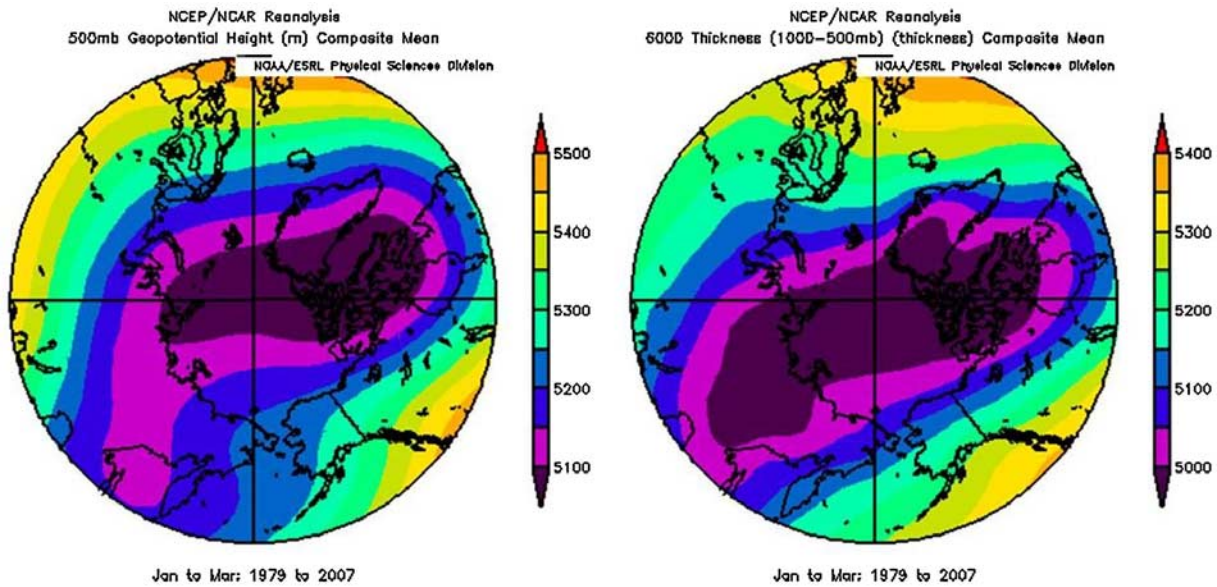


Figure 3. (left) Mean (1979–2007) 500 hPa geopotential height field for winter. (right) The 500–1000 hPa geopotential thickness field, proportional to mean layer temperature for the same period.

how this is manifest monthly and regionally is more complicated. One of misunderstandings in previous Arctic climatologies, evident in Figure 2, is that there is not a year-round semipermanent anticyclone (a closed region of high SLP), the Beaufort high. In winter the cold surface and low geopotential heights aloft give a ridge of high SLP spanning the Beaufort Sea from Siberia to Alaska/Canada. It is only in the autumn and spring, when the upper air polar vortex is not as well developed but the surface is still cold, that a Beaufort High SLP is evident. In summer the SLP field is a rather flat over the Beaufort Sea with a low SLP center near the Pole, which suggests that there is little control of surface conditions by large scale hemispheric climate patterns; the local heat and moisture balance and the intermittent presence of smaller weather systems are important.

[8] The 500 hPa geopotential height field for winter from more recent data, along with the surface to 500 hPa geopotential thickness field proportional to mean layer temperature, reconfirms *Hare's* [1968] conjecture that the lower atmosphere in winter is dominated by a cold core polar vortex (Figure 3). The 850 hPa geopotential height field for summer shows a rather flat distribution, again reinforcing the concept of weak midlevel atmospheric control of surface conditions (Figure 4).

[9] The annual cycle of air temperature at the SHEBA site in the middle of the Beaufort Sea is shown in Figure 5. Near surface (10 m height) temperatures in winter (black line) vary between -25° and -40°C , depending on cloud cover. Clouds provide a greenhouse-like blanket which traps the heat near the surface which can rapidly elevate the surface temperature by 10°C or more compared to clear sky conditions. For summer, there is a unique situation for Polar regions; temperatures are near 0°C with extra heat going into melting snow and sea ice, keeping the temperature near the sea ice melting point, a water-ice bath. The SHEBA year temperatures are close to the climatological Arctic basin temperatures based on the multiyear North Pole drifting

stations, which show December to February mean temperatures near -33°C [Frolov *et al.*, 2005].

[10] The Arctic is known for stable stratification in the planetary boundary layer, the region influenced by surface conditions, which tends to decouple the surface winds from stronger flow aloft. During winter most days are characterized by surface “inversions” where the temperature increases with height. The air is strongly stable relative to the adiabatic rate of temperature decrease with height. The vertical profiles of temperature observed at SHEBA shown

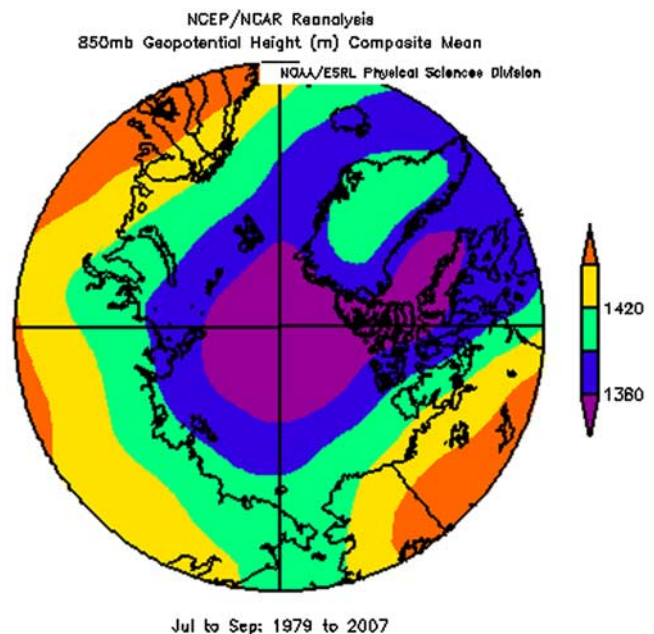


Figure 4. Geopotential height field for 850 hPa during summer.

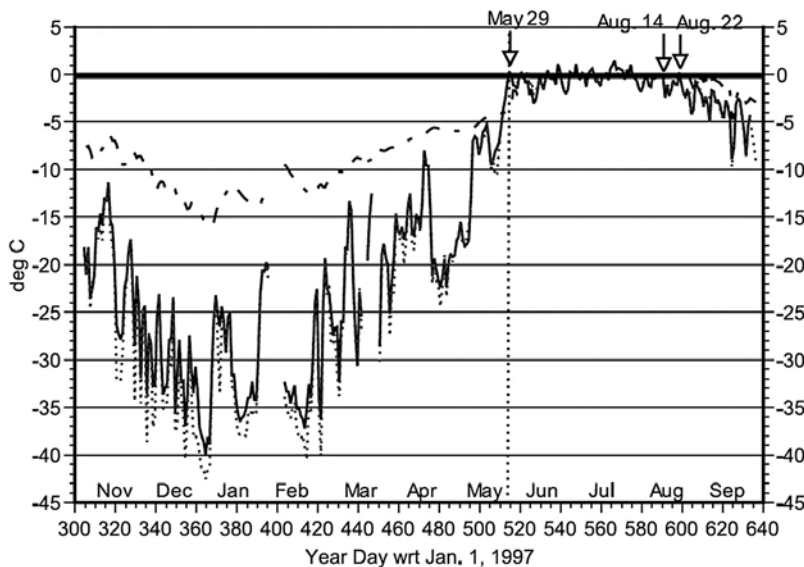


Figure 5. Near-surface conditions at the SHEBA site. Shown are daily mean values of 10-m air temperature (solid curve), surface temperature (dotted curve), and ice/snow interface temperature (dot-dashed curve). After *Persson et al.* [2002].

in Figure 6a are “normalized,” which means that the vertical axis is scaled by the height where the temperature becomes constant with height (dashed line), which is typically at 200–700 m above the surface, and the temperature is centered on the observed mean temperature below this height [Tjernstrom and Graversen, 2009]. Vertical temperature differences across the boundary layer are large, on the order of 10°C, and different days have similar profiles. During October through March during the SHEBA year, 56% of the soundings had this structure, while only 11% of the soundings from April through September had such a surface based inversion. Radiative equilibrium maintains this low level temperature difference, because the emissivity of the atmospheric temperature maximum layer, the region just above the scaling height, is less than the snow surface. The temperature at the level of the temperature maximum generally depends on atmospheric advection over large horizontal spatial scales (~1000 km). Such a unique temperature maximum/surface inversion structure was termed a “radiative boundary layer” by *Overland and Guest* [1991].

[11] In summer the temperature profiles are scale by the height that a surface based nearly well mixed layer is capped by the beginning of a major increase in temperature with height, the inversion base (Figure 6b). During SHEBA the summer inversion bases were typically at 200–400 m above the surface [Tjernstrom and Graversen, 2009]. This well mixed structure can exist in summer because the radiative heat loss from the surface is no longer the dominant physics in the boundary layer. These elevated inversions were present (89%) for most of the summer half of the year at SHEBA.

[12] The annual cycle of cloud characteristics were observed at the SHEBA camp via radar and lidar sensors [Intrieri et al., 2002]. They show an average cloud occurrence for December through February of 68% and for April through August of 92%. These values are greater than those

from earlier climatologies using visual observations (47 and 83%) or derived from satellites (60 and 80%). Clouds warm the surface for most of the year with a brief period of cooling in the middle of summer [Intrieri et al., 2002].

3. Energy Fluxes

[13] The region of the Arctic Ocean must import heat from the south due to the net radiation loss to space from the top of the atmosphere. It acts as the primary energy sink for the heat engine of the Earth and establishes north–south temperature gradients which drive the general circulation of the atmosphere. The large scale energy budget of the Arctic Ocean as a whole has recently been reviewed by *Serreze et al.* [2007a], and the surface energy budget observed at SHEBA is given by *Persson et al.* [2002]. The January and July energy budget of the Arctic Ocean north of 70°N is shown in Figure 7, based on using ERA-40 Reanalysis fields [Serreze et al., 2007a]. At the top of the atmosphere the long wave energy (LW) loss is ~230 W/m² in summer and ~180 W/m² in winter, while short wave (SW) flux is ~240 W/m² downward, only in summer. The transfer of energy from the south into the Arctic (given by $-\nabla \bullet F$) is about the same for summer and winter, ~80–90 W/m². These two external forcings, radiative and advective, give a net increase in energy into the ocean in July of ~100 W/m² associated with sea ice melt and sensible heat, while in January the surface has a net loss of ~60 W/m². In winter the radiative loss at the top of the atmosphere is about equal to the sum of the contributions from radiative loss at the surface and horizontal advection, the Arctic contribution to the heat engine of the planet. These results should be qualitatively similar for the Beaufort Sea region, except as noted below.

[14] Energy fluxes at the surface in the Beaufort Sea for the SHEBA year are shown in Figure 8. In Figure 8a, F_{tot} is the total vertical heat flux and Q^* is the sum of the

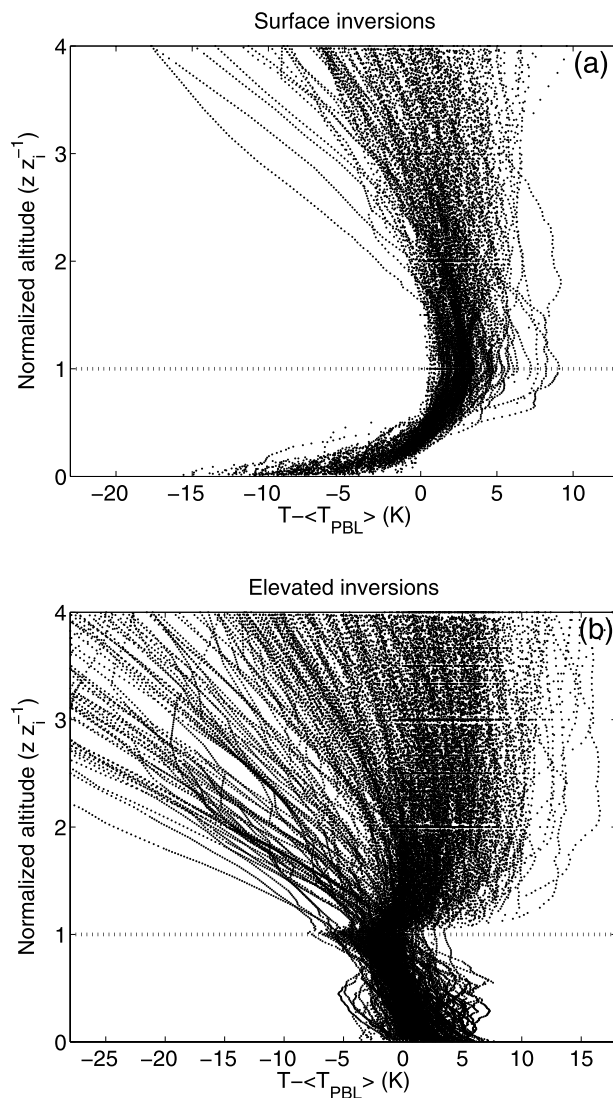


Figure 6. Normalized temperature profiles for (a) winter surface and (b) summer-elevated inversions from the SHEBA soundings. The vertical scale is normalized by the boundary layer depth, here taken from the temperature inversions. Normalized temperature profiles are formed by subtracting the mean boundary layer temperature from the actual values. After *Tjernstrom and Graversen* [2009]. © Royal Meteorological Society.

longwave and shortwave contributions, separated out in Figure 8b as Q_s and Q_l . Albedo is α , H_s and H_l are sensible and latent heat flux, and C is the conductivity flux from the ocean through the sea ice to the surface. At the SHEBA site, the total surface flux varied from -25 to $+12$ W/m^2 in winter to $+37$ to $+129$ W/m^2 in July [*Persson et al.*, 2002]. Most variability is from changes in cloud cover. These numbers are considerably smaller than the Arctic-wide estimates by *Serreze et al.* [2007a] in Figure 7, but the Arctic-wide estimates include additional sensible heat flux from open water areas in the Atlantic sector north of $70^\circ N$. As in the Arctic-wide estimates, radiative terms dominate the surface energy budget in winter and summer; turbulent fluxes are 5–10 times smaller, and generally

oppose the effect of net radiation. By October, accumulation of excess energy, *Ftot-run_mean*, was equivalent to melting of nearly 1 m of sea ice.

4. Near and Far Past and the Near Future

[15] How stable is the climate of the Beaufort Sea? Figure 9 shows the monthly anomalies of surface air temperature (SAT) and SLP from 1950 through 2007 for the Beaufort Sea, averaged over 130 – $160^\circ W$ and 72 – $82^\circ N$, i.e., the region above the deep ocean basin. Labels on Figure 9 (bottom) refer to month of the year, and the vertical scale is the yearly time axis. Anomalies are calculated relative to a 1951–2000 base period for each month. Recall that data to form these estimates is minimal or lacking before 1979. The Beaufort was clearly warmer than the long-term record throughout the year from the late 1990s onward with several monthly anomalies of greater than $4^\circ C$. These increased temperatures were also Arctic-wide and contain a global warming component [*Serreze et al.*, 2007b; *Overland et al.*, 2008]. Summers were slightly colder before the mid-1990s back to 1961. The decade of the 1960s was particularly cool. The SLP anomalies show considerable month to month and year to year variability. Higher than normal SLP are observed from 2004 to 2006 in spring and for 2007 in summer. Lower SLP is observed in winter from 1989 through the mid-1990s and in the mid-1970s.

[16] In deeper history, various proxies imply an interval of warmer than present temperatures of $+2$ – $3^\circ C$ for the coastal plain of Alaska in the early Holocene, between 11,500 and 9000 years before present [*Kaufman et al.*, 2004]. This warming occurred earlier than in the remainder of North America, because the Laurentide glacial ice sheet was still centered toward the central and eastern half of the continent. The range of bowhead whales, adapted to live along the ice edge of the Beaufort Sea, has expanded and contracted abruptly several times over the last 10,500 years [*Dyke et al.*, 1996]. Bowhead populations from 10,500 to 8500 years before present (BP) had a range in summer from the Beaufort Sea through to Baffin Bay. For 8500 to 5000 BP, bowheads were excluded from the Canadian Archipelago with more severe ice cover than in modern times. For 5000 to 3000 BP bowheads reoccupied the central channels of the Arctic Islands beyond historical limits, while from 3000 BP to present they are excluded from these channels by sea ice. In the last 700 years it was mainly cold from 1240 to 1520 and 1730–1920 and warm from 1520 to 1730 and after 1920, based on analysis of pollen taken from 9 lake cores near Barrow, Alaska [*Tang et al.*, 2003].

[17] As suggested by the SAT plot in Figure 9, the meteorology and sea ice conditions were different for the beginning of the 21st century compared with the second half of the twentieth century. The circulation of the sea ice cover and ocean surface layer are closely coupled and are primarily wind-driven. Data from satellites and drifting buoys indicate that the entire period of 1997–2007 has been characterized by an anomalous anticyclonic (clockwise) sea ice circulation regime. The Arctic Ocean Oscillation index (AOO [*Proshutinsky and Johnson*, 1997]) predicts the central Arctic upper ocean circulation based on sea level height at the edge of the Beaufort ocean gyre using an ocean model driven by surface winds. The major

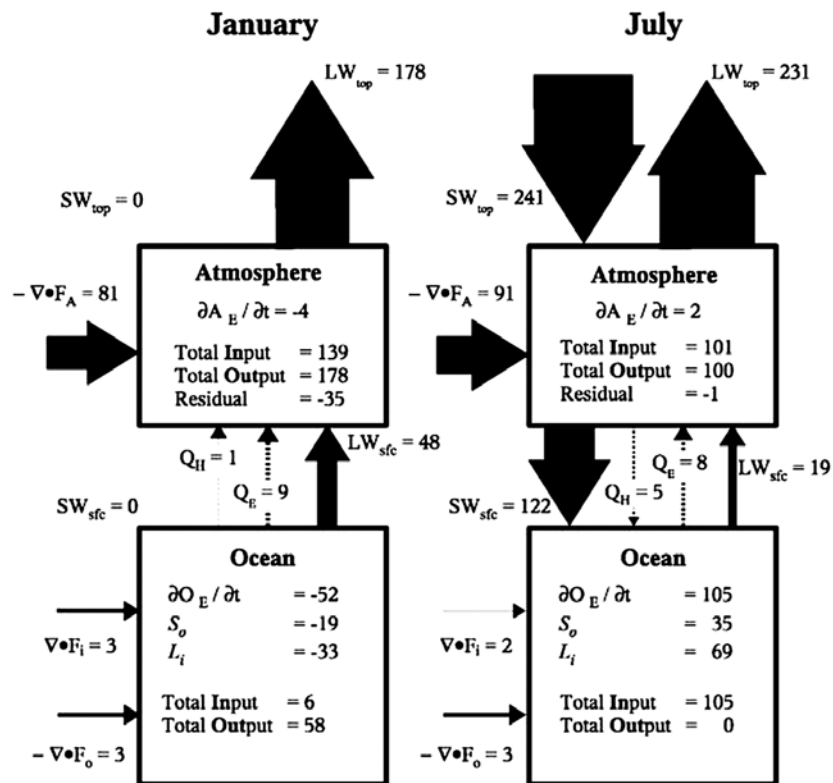


Figure 7. Schematic of the Arctic energy budget for January and July [after Serreze *et al.*, 2007a]. Symbols are defined in the text. Units are in W/m^2 . The width of the arrows is proportional to the size of the transports.

characteristics of this index (Figure 10, bottom) demonstrate that indeed during 1997–2007 (positive AOO index, blue bars) the Arctic Ocean circulation regime was anticyclonic. Moreover, in 2004 and 2007 this index was as much as two times larger than its maximum throughout 1948–2000. Climatologies are classically based on averages over 30 years of record. On the basis of Figure 10, however, it is more appropriate to classify Beaufort Sea climate events by whether they occur in positive or negative AOO intervals.

[18] During the twentieth century it was recognized that the Arctic Oscillation (AO [Thompson and Wallace, 1998]) index of SLP variability for the Northern Hemisphere (Figure 10, bottom, black line) is an indicator of Arctic atmosphere circulation regimes, and as expected was generally out of phase with the AOO, i.e., a high AO index is associated with lower SLP over the Arctic and cyclonic wind-forcing. Over the last decade, however, the AO exhibited relatively low and fluctuating values. The dominance of the AO was generally replaced by a more meridional atmospheric flow with anomalous winds blowing from the Bering Sea toward the North Pole, supporting a positive AOO for the Beaufort Sea [Overland *et al.*, 2008]. The positive AO of the early 1990s followed by nearly a decade of the unusual meridional flow pattern has led to decreases in sea ice thickness throughout the Arctic [Nghiem *et al.*, 2007].

[19] In 2007 the meridional wind pattern was also seen in summer, with high SLP over the Beaufort side of the Arctic Basin and low SLP on the Siberian side, which strongly supported the Beaufort AOO anticyclonic mode. Sea ice

coverage in September 2007 was 37% below its climatology from the 1990s, with half of this loss observed in one year. Perhaps the largest impact from this sea ice loss is the effect of open water on higher autumnal temperatures over most of the Arctic (Figure 11). Most of the central Arctic was over $6^\circ C$ above normal for October/November during 2005–2007. This extra atmospheric and ocean heat has to be removed before sea ice growth rates can return to typical values; the impact of warmer temperatures shortens the total time available in winter to grow ice, providing a potential year to year memory for ice loss.

[20] The loss of multiyear sea ice and the warm fall temperatures suggest that it would be difficult to quickly return to 1980s conditions in the Beaufort Sea, even when the AO pattern of climate variability eventually reasserts itself. The Arctic seems to be on a fast track for warmer temperatures and sea ice loss due to a weak global warming signal, the fortuitous timing of the intrinsic atmospheric climate patterns (positive AO followed by the meridional pattern), and the effect of nonlinear feedbacks from increased open water area initiated by the first two factors. However, we should still expect much interannual and decadal variability in the near future due to the large possible range of natural atmospheric circulation patterns.

5. Summary

[21] The unique meteorology of the Beaufort Sea region is caused by the presence of sea ice and a seasonal swing from a large heat loss in winter to a gain in summer. Even

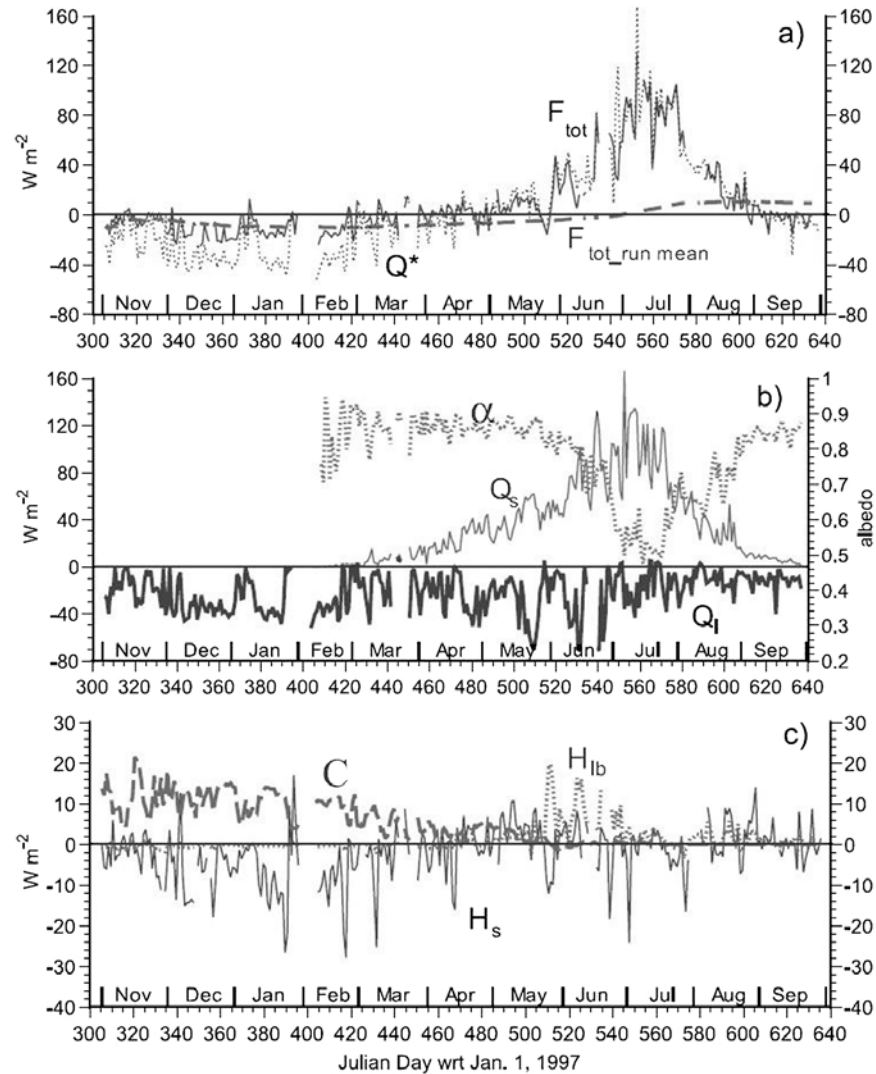


Figure 8. Surface energy budget at the SHEBA camp site [after Persson *et al.*, 2002]. (a) F_{tot} is the total vertical heat flux, and Q^* is total radiative flux; (b) Q_s is the shortwave and Q_l is the longwave contribution. Albedo is α . (c) H_s and H_{lb} are sensible and latent heat flux, and C is the conductivity flux from the ocean through the sea ice to the surface. The cumulative mean for F_{tot} on 1 November 1997.

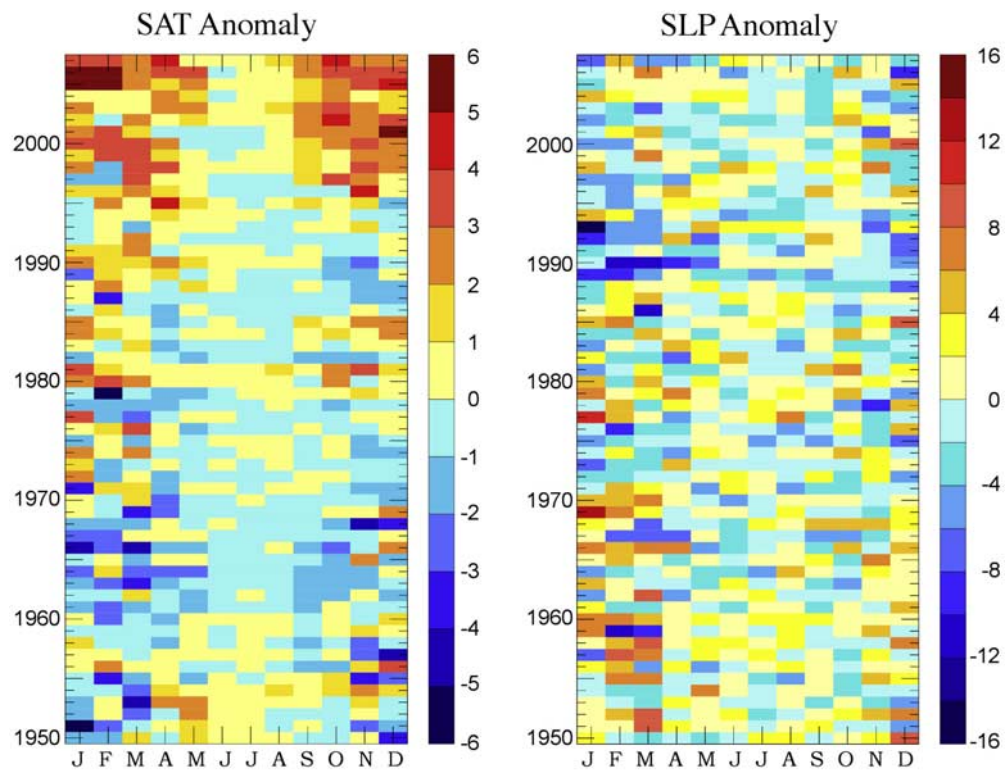


Figure 9. Surface air temperature (SAT) and SLP anomalies for each month of the year (x axis) for sequential years (y axis). Monthly values are from the NCEP/NCAR reanalysis. The base period is 1951–2000 for each month.

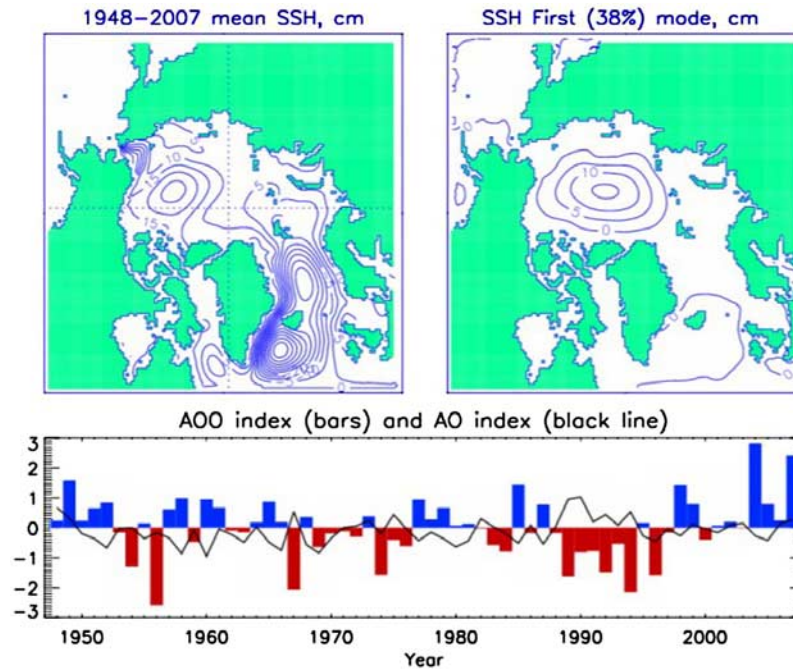


Figure 10. (top left) The 1948–2007 mean structure of sea surface heights (SSH) generated by atmospheric winds in an idealized wind-driven circulation model of the Arctic Ocean [Proshutinsky and Johnson, 1997]. (top right) The first EOF mode (38% of variance) of SSH based on analysis of annual simulated sea surface heights in the region, showing that the main pattern of variability is a strengthening or weakening of the anticyclonic gyre. (bottom) Time series of the first mode of the Arctic Ocean Oscillation (AOO) index (bars) and the Arctic Oscillation (AO) index (black line). There are persistent periods with the AOO of predominately one sign or the other (blue/red). Since approximately 1997, the anticyclonic [clockwise, positive (blue) AOO index] circulation regime dominates the central Arctic Ocean with elevated sea surface height relative to norm. This means that the Beaufort Gyre High expands (propagating north) and involving the entire Arctic Ocean in the anticyclonic rotation. Figure 10 is a new update of the original Proshutinsky and Johnson [1997] simulation extending their analysis for 1948–2007 and was prepared by A. Y. Proshutinsky (personal communication, 2008).

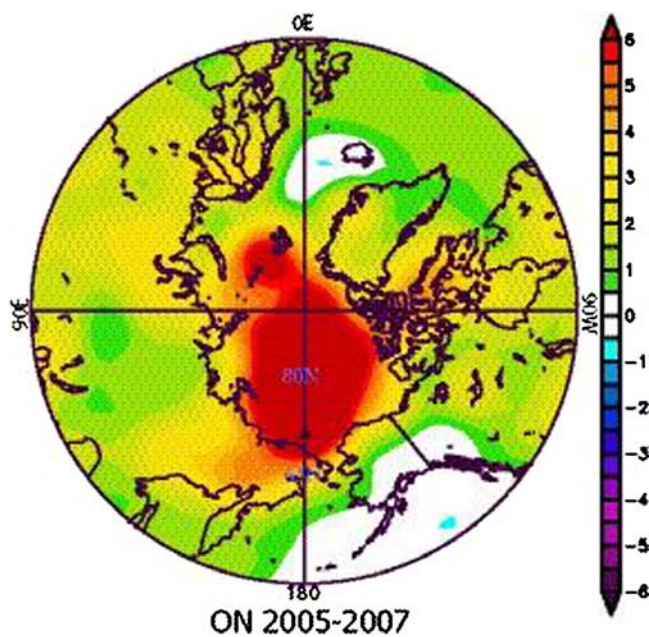


Figure 11. Autumn (ON) surface air temperature anomalies averaged for 2005–2007. Central Arctic values are greater than $+6^{\circ}\text{C}$.

though the Sun angle is low in summer, the length of daylight provides as much energy to the surface as anywhere on the planet. This annual cycle results in a change from a winter continental-like air mass similar to the adjacent land areas to a summertime marine air mass characterized by low cloud and fogs. The winter radiation deficit at the surface combined with atmospheric advection from the south leads to a surface based inversion vertical temperature structure, the radiative boundary layer. In winter the region is also influenced by the polar atmospheric vortex with strong westerly winds centered in the stratosphere, whose presence is felt at the surface.

[22] Recent sea ice losses are changing the climatology of the region, especially with increased temperatures through the autumn months of greater than 6°C . The loss of multiyear sea ice and the warm fall temperatures suggest that it would be difficult to quickly return to pre-1990 conditions in the Beaufort Sea.

[23] **Acknowledgments.** We appreciate the support from the NOAA Arctic Research in preparation of this paper. M. Wang helped with the preparation of Figures 1–11. The review was made possible by the many accomplishments of Arctic scientists in the last decade and beyond, as

noted in the References and elsewhere. This paper is dedicated to the memory of Richard Reed, author of the 1960 paper on the summer Arctic.

References

- Dyke, A. S., J. Hopper, and J. M. Saville (1996), A history of sea ice in the Canadian Arctic Archipelago based on postglacial remains of bowhead whale, *Arctic*, *49*, 235–255.
- Frolov, I. E., et al. (2005), *The Arctic Basin*, 272 pp., Springer, Chichester, U. K.
- Hare, F. K. (1968), The Arctic, *Q. J. R. Meteorol. Soc.*, *94*, 439–459.
- Intrieri, J. M., M. D. Shupe, T. Uttal, and B. J. McCarty (2002), An annual cycle of Arctic cloud characteristics observed by radar and lidar at SHEBA, *J. Geophys. Res.*, *107*(C10), 8030, doi:10.1029/2000JC000423.
- Kaufman, D. S., et al. (2004), Holocene thermal maximum in the western Arctic (0–180 W), *Quat. Sci. Rev.*, *23*, 529–560.
- Makshas, A., D. Atkinson, M. Kulakov, S. Shutilin, R. Krishfield, and A. Proshutinsky (2007), Atmospheric forcing validation for modeling the central Arctic, *Geophys. Res. Lett.*, *34*, L20706, doi:10.1029/2007GL031378.
- Nghiem, S. V., I. G. Rigor, D. K. Perovich, P. Clemente-Colón, J. W. Weatherly, and G. Neumann (2007), Rapid reduction of Arctic perennial sea ice, *Geophys. Res. Lett.*, *34*, L19504, doi:10.1029/2007GL031138.
- Overland, J. E., and P. S. Guest (1991), The Arctic snow and air temperature budget over sea ice during winter, *J. Geophys. Res.*, *96*, 4651–4662.
- Overland, J. E., M. Wang, and S. Salo (2008), The recent Arctic warm period, *Tellus, Ser. A*, *60*, 589–597.
- Persson, P. O. G., C. W. Fairall, E. L. Andreas, P. S. Guest, and D. K. Perovich (2002), Measurements near the atmospheric surface flux tower at SHEBA: Near-surface conditions and surface energy budget, *J. Geophys. Res.*, *107*(C10), 8045, doi:10.1029/2000JC000705.
- Proshutinsky, A. Y., and M. Johnson (1997), Two circulation regimes of the wind driven Arctic Ocean, *J. Geophys. Res.*, *102*, 12,493–12,514.
- Reed, R. J., and B. A. Kunkel (1960), The Arctic circulation in summer, *J. Meteorol.*, *17*, 489–506.
- Serreze, M. C., and R. G. Barry (2006), *The Arctic Climate System*, 385 pp., Cambridge Univ. Press, Cambridge, U.K.
- Serreze, M. C., A. P. Barrett, A. G. Slater, M. Steele, J. Zhang, and K. E. Trenberth (2007a), The large-scale energy budget of the Arctic, *J. Geophys. Res.*, *112*, D11122, doi:10.1029/2006JD008230.
- Serreze, M. C., M. M. Holland, and J. Stroeve (2007b), Perspectives on the Arctic's shrinking sea-ice cover, *Science*, *315*, 1533–1536.
- Tang, L., et al. (2003), Study on climate change in pollen records in Barrow Arctic, and compared with the Tibetan Plateau since 13th century, *J. Glaciol. Geocryol.*, *25*, 261–267.
- Thompson, D. W. J., and J. M. Wallace (1998), The Arctic Oscillation signature in the wintertime geopotential height and temperature fields, *Geophys. Res. Lett.*, *25*, 1297–1300.
- Tjernstrom, M., and R. G. Graversen (2009), The vertical structure of the lower Arctic troposphere analysed from observations and ERA-40 reanalysis, *Q. J. R. Meteorol. Soc.*, in press.
- Uttal, T., et al. (2002), Surface heat budget of the Arctic Ocean, *Bull. Am. Meteorol. Soc.*, *255*–275.
- Vangengeim, G. Y. (1946), On variations in the atmospheric circulation over the Northern Hemisphere, *Izv. SSSR, Ser. Geogr.*, *5*.
- Vangengeim, G. Y., and A. F. Laktionov (1967), *The Hydrometeorology of the Polar Regions, Tr. Arkt. Antarkt. Nauchno Issled. Inst.*, *253*, 280 pp.
- Vowinckel, E., and S. Orvig (1970), The climate of the North Polar Basin, in *Climate of the Polar Regions, World Surv. Climatol.*, vol. 14, edited by S. Orvig, pp. 129–252, Elsevier, New York.

J. E. Overland, Pacific Marine Environmental Laboratory, NOAA, Seattle, WA 98115, USA. (james.e.overland@noaa.gov)